

References and Notes

- (1) Part 49: M. J. S. Dewar, S. Olivella, and H. Rzepa, *J. Am. Chem. Soc.*, **100**, 5650 (1978).
- (2) See: H. C. Brown, "Hydroboration", Benjamin, New York, N.Y., 1962.
- (3) See: H. C. Brown, "Boranes in Organic Chemistry", Cornell University Press, Ithaca, N.Y., 1972, pp 209–251.
- (4) See: R. B. Woodward and R. Hoffmann, *Angew. Chem., Int. Ed. Engl.*, **8**, 781 (1969).
- (5) See: M. J. S. Dewar, *Angew. Chem., Int. Ed. Engl.*, **10**, 761 (1971).
- (6) M. J. S. Dewar and W. Thiel, *J. Am. Chem. Soc.*, **99**, 4899, 4907 (1977).
- (7) R. C. Bingham, M. J. S. Dewar, and D. H. Lo, *J. Am. Chem. Soc.*, **97**, 1285, 1294, 1302, 1307 (1975).
- (8) M. J. S. Dewar and M. L. McKee, *J. Am. Chem. Soc.*, **99**, 5231 (1977).
- (9) M. J. S. Dewar and M. L. McKee, *Inorg. Chem.*, in press.
- (10) M. J. S. Dewar and M. L. McKee, *J. Am. Chem. Soc.*, in press.
- (11) M. J. S. Dewar and M. L. McKee, *Inorg. Chem.*, **17**, 1075 (1978).
- (12) A. Komornicki and J. W. McIver, Jr., *J. Am. Chem. Soc.*, **95**, 4512 (1973).
- (13) M. J. S. Dewar and G. P. Ford, *J. Am. Chem. Soc.*, **99**, 8343 (1977).
- (14) D. J. Pato and B. Lepeska, *J. Am. Chem. Soc.*, **98**, 1091 (1976).
- (15) H. C. Brown and K. Ichikawa, *J. Am. Chem. Soc.*, **83**, 4372 (1961).
- (16) E. C. Ashby and J. R. Boone, *J. Am. Chem. Soc.*, **98**, 5524 (1976).
- (17) J. L. Pierre and H. Handel, *Tetrahedron Lett.*, 2317 (1977).
- (18) D. C. Wigfield and F. W. Gowland, *J. Org. Chem.*, **42**, 1108 (1977).
- (19) C. Adams, V. Gold, and D. M. E. Reuben, *J. Chem. Soc., Perkin Trans. 2*, 1466 (1977).
- (20) D. C. Wigfield, S. Feiner, and F. W. Gowland, *Tetrahedron Lett.*, 3377 (1976).
- (21) R. E. Davis, E. Bromels, and C. L. Kibby, *J. Am. Chem. Soc.*, **84**, 885 (1962).
- (22) T. P. Fehlner, *Inorg. Chem.*, **11**, 252 (1972); *J. Phys. Chem.*, **76**, 3532 (1972).
- (23) This mechanism was suggested by P. R. Jones, *J. Org. Chem.*, **37**, 1886 (1972).
- (24) M. J. S. Dewar, E. A. C. Lucken, and M. A. Whitehead, *J. Chem. Soc.*, 2423 (1960).
- (25) M. J. S. Dewar, "The Molecular Orbital Theory of Organic Chemistry", McGraw-Hill, New York, N.Y., 1969, pp 140, 143, 430.
- (26) M. J. S. Dewar and R. C. Dougherty, "The PMO Theory of Organic Chemistry", Plenum Press, New York, N.Y., 1975, section 3.6; ref 25, section 5.5.
- (27) M. G. Evans and E. Warhurst, *Trans. Faraday Soc.*, **34**, 614 (1938); M. G. Evans, *ibid.*, **35**, 824 (1939).
- (28) J. A. Ross, R. P. Sieders, and D. M. Lemal, *J. Am. Chem. Soc.*, **98**, 4325 (1976).
- (29) D. P. Craig, *J. Chem. Soc.*, 997 (1959).
- (30) M. J. S. Dewar, *J. Am. Chem. Soc.*, **74**, 3345 (1952).
- (31) M. J. S. Dewar, *Tetrahedron Suppl.*, **8**, 75 (1966).
- (32) E. Heilbronner, *Tetrahedron Lett.*, 1923 (1964).
- (33) H. E. Zimmerman, *J. Am. Chem. Soc.*, **88**, 1564 (1966).

ENDOR of Organic Triplet- and Quartet-State Molecules in Liquid Solutions and in Rigid Media

B. Kirste,^{1a} H. van Willigen,[†] H. Kurreck,^{*1a}
K. Möbius,^{1b} M. Plato,^{1b} and R. Biehl[‡]

*Contribution from the Institut für Organische Chemie and the
Institut für Molekülphysik, Freie Universität Berlin,
1000 Berlin 33, West Germany. Received March 24, 1978*

Abstract: ESR, ENDOR, electron-nuclear-triple resonance (TRIPLE), and ENDOR-induced ESR measurements have been performed on a variety of phenoxyl-type biradicals and triradicals in isotropic fluid solutions and in rigid media. The free nuclear frequency absorption lines, previously predicted for triplet-state molecules, could readily be detected in the rigid-matrix ENDOR spectra of the biradicals. For the first time the fluid-solution and rigid-media ENDOR spectra of triradicals in the quartet spin state could be obtained. The unambiguous assignment of the resonance lines to the respective spin states was achieved by using TRIPLE and ENDOR-induced ESR techniques. The signs of the zero-field splitting parameters D could be determined relative to those of the hyperfine couplings thus providing some structural conclusions for the radicals under study. A qualitative outline of the dependence of the spin relaxation processes on the electron–electron dipolar interaction of the multispin systems is given.

Introduction

In recent years there has been considerable interest in studying organic multispin systems by means of electron spin resonance (ESR).² Unfortunately, most of the isotropic solution ESR spectra are only poorly resolved due to the anisotropic electron–electron dipolar interaction (zfs) which often exceeds 100 MHz and is then no longer averaged out by the Brownian motion. Moreover, the exchange interaction, also present in all multispin systems, reduces the hyperfine splittings as compared to those of the corresponding monoradicals. It therefore appeared promising to apply the electron nuclear double resonance (ENDOR) technique with its larger resolving power.

Recently³ we reported the first successful ENDOR experiments on some galvinoxyl biradicals in liquid solution. Apart from being able to resolve hyperfine splittings not yet observed by ESR, the most remarkable result was the absence of the line at the free proton frequency ν_p expected for biradicals such as

Yang's biradical (**1c**) in which the exchange integral J is much larger than the hyperfine coupling. This " ν_p line" was expected to arise from NMR transitions within the $M_S = 0$ electron spin manifold. Actually it was the absence of this line which in some cases prevented the unambiguous assignment of the ENDOR spectrum to a biradical. The failure to observe the ν_p line could be explained by considering that, in liquid solution, the ESR transitions $|-1, M_I\rangle \leftrightarrow |0, M_I\rangle$ and $|0, M_I\rangle \leftrightarrow |1, M_I\rangle$ are degenerate within the ESR line width. Therefore both transitions are pumped equally strongly thus leaving the thermal nuclear spin polarization in the $M_S = 0$ manifold undisturbed.

Alternatively, one would expect the ν_p line to show up in a rigid-matrix ENDOR spectrum since the degeneracy of the ESR transitions is now lifted by the electron–electron dipolar interaction. The present communication contains a detailed report and discussion of our biradical studies in rigid matrices. We have reported on ENDOR measurements on some carbon-13-labeled galvinoxyl biradicals in rigid media.⁴

For a quartet-state molecule with $S = 3/2$ and $|J| \gg |a|$ one expects a distinctly different behavior of the transitions $|3/2, M_I\rangle \leftrightarrow |1/2, M_I\rangle$ and $|-3/2, M_I\rangle \leftrightarrow |-1/2, M_I\rangle$ on the one hand

[†] Department of Chemistry, University of Massachusetts, Boston, Mass. 02125.

[‡] Bruker Physik AG, Am Silberstreifen, 7512 Karlsruhe, Germany.

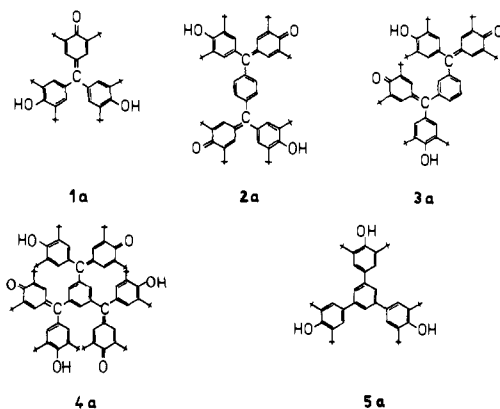


Figure 1. Numbering scheme of compounds: **a**, galvinoxyls or phenols; **b**, monoradicals (first oxidation steps); **c**, biradicals (second oxidation steps); **d**, triradicals (third oxidation steps).

and the transition $|-\frac{1}{2}, M_I\rangle \leftrightarrow |+\frac{1}{2}, M_I\rangle$ on the other hand with regard to broadening and saturation effects since these two types of transitions are differently affected by the electron-electron dipolar interaction. This will not be resolved in a solution ESR spectrum which consists of a superposition of all transitions but should manifest itself in rigid-matrix ESR and liquid and matrix ENDOR spectra. ENDOR lines can be observed separately in the individual M_S manifolds, and in the matrix it is possible to pump selectively the two different types of ESR transitions.

The multispin ENDOR study in a rigid matrix provides a unique opportunity to probe the ENDOR effect not only within different electron spin (M_S) manifolds but also for different radical orientations although one is dealing with randomly oriented samples. Unlike the fluid-solution studies, ENDOR in frozen solution should, in principle, yield the relative signs of zero-field splitting (zfs) and hyperfine coupling constants.

As a variation of ENDOR, ENDOR-induced ESR⁵ has proved to be useful for separating overlapping ESR spectra arising from different radicals. In the field of multispin systems this technique may serve to discriminate between the spectra belonging to different ESR transitions.

In the investigation of multispin systems particular care has to be taken to identify the nature of the compound under study, because different electronic spin state species might exist simultaneously for chemical (oxidation step) or physical reasons (thermal quartet-doublet equilibrium in triradicals). Electron-nuclear-nuclear-triple resonance (TRIPLE)⁶ should be able to ensure the assignment of ENDOR lines to specific species.

In this paper we shall report on ENDOR, ENDOR-induced ESR, and TRIPLE measurements on some phenoxyl radicals in the electronic triplet and quartet spin states in isotropic fluid solutions and in rigid media. To our knowledge no ENDOR experiments on biradicals in rigid media and on triradicals both in fluid solution and in rigid media have been reported to date.

Experimental Section

Preparation of Compounds. All of the galvinoxyl precursors **1a–4a** were obtained following our organometallic synthetic pathway described elsewhere⁷ yielding mono- and oligogalvinoxyls; see Figure 1.

The galvinoxyl radicals were prepared on a vacuum line by treating carefully degassed solutions of the galvinoxyls with lead dioxide in the ESR/ENDOR sample tube. For a more detailed description see ref 8.

Phenoxyls **5b–5d** were prepared in a similar manner from the corresponding tris(phenol) **5a**.⁹

Instrumentation. ESR, ENDOR, ENDOR-induced ESR, and

general TRIPLE spectra were recorded with a modified Varian E12 ESR spectrometer,¹⁰ an AEG-12 X ESR spectrometer, and an AEG-20 XT spectrometer with an ENDOR accessory. Measurements were performed on solutions of the radicals in toluene, 2-methyltetrahydrofuran (MTHF), paraffin oil, or liquid crystal phase IV (Merck). Calculations were performed with a CDC Cyber 175 computer system with a STATOS Plotter 3313.

Results and Discussion

Biradicals (Triplet-State Molecules). Fluid-Solution ENDOR Measurements. For a biradical in which the exchange interaction J is much larger than the hyperfine couplings each set of equivalent nuclei, in principle, can give rise to three ENDOR lines.¹¹ This is predicted by the resonance condition $\nu_{\text{ENDOR}} = |\nu_N - M_S a_i^T|$ with $M_S = -1, 0, \text{ or } +1$, where ν_N is the free nuclear frequency and a_i^T the triplet coupling parameter. The value of a_i^T is given by the distance of two adjacent hyperfine components in the biradical ESR spectrum belonging to one group of equivalent nuclei. In practice the ν_N line is not observed in fluid-solution ENDOR since pumping of the ESR transitions generally does not result in nuclear spin polarization in the $M_S = 0$ manifold.³ Theoretical work indicates that the line may become observable if a strong cross-relaxation mechanism operates in the biradical.¹² So far we have not come across an example where that condition is fulfilled. The ν_N line may also show up in TRIPLE experiments. General TRIPLE has been applied on Yang's biradical **1c** in fluid solution, but no ν_p line was observed. Possibly the applied microwave and radio-frequency fields were not sufficiently strong to produce the desired effect.

Rigid-Matrix ENDOR Measurements. In most cases the rigid-matrix ESR spectra of biradicals with $|J| \gg |a|$ exhibit regions where pairs of transitions $| -1, M_I \rangle \leftrightarrow | 0, M_I \rangle$ and $| 0, M_I \rangle \leftrightarrow | 1, M_I \rangle$ are clearly separated on account of the zero-field splitting, since this interaction is no longer averaged out as in liquid solution.¹³ As a consequence, the ν_p line now should be observable in the ENDOR experiment. Actually all biradicals investigated give a signal at ν_p , when the solvent (toluene, MTHF, paraffin oil) is frozen into a matrix. The line width of this signal is generally about 20 kHz which is exceptionally narrow for an ENDOR line of a free radical randomly distributed in a rigid matrix. Note, for instance, that the line width is comparable to the minimum proton ENDOR line width of ca. 40 kHz found for radicals in fluid solution.¹⁴ Such a narrow line width is atypical for solvent protons in the vicinity of the biradical.¹⁵ That the ν_p signal must stem from the biradical itself is established by the fact that the signal is also observed when the biradical is prepared in perdeuteriotoluene. Additional support is obtained by the ENDOR-induced ESR measurements; vide infra. The signal amplitude decreases gradually as the temperature increases. This decrease is not due to a line-width increase but must be attributed to the loss of nuclear spin polarization as the zfs is averaged out.

Additional evidence of the origin of the ν_p signal can be gained from two more facts: (i) the line width is roughly one order of magnitude smaller than the fluid-solution biradical ENDOR line width³ and (ii) the line width does not depend on the magnetic field setting. The contrary would be expected for the states $M_S = \pm 1$ for which the range of orientations being probed is strongly field dependent thus giving rise to varying line-widths contributions from the anisotropy of the hyperfine interaction.¹⁶ All of these observations lead to the only possible conclusion that the ν_p signal originates from NMR transitions in the state $M_S = 0$.

Table I shows that the D and E values of the biradicals investigated are much smaller than the Zeeman interaction. This means that the admixture of the $M_S = 1, 0, \text{ and } -1$ electron spin functions by the electron spin-electron spin interaction is negligibly small irrespective of the orientation of the biradical with respect to the field direction. Since the hyperfine couplings

Table I. *g*- and *D*-Tensor Values of the Bi- and Triradicals

compd	<i>D</i> , MHz	<i>E</i> , MHz	<i>g</i> _{xx}	<i>g</i> _{yy}	<i>g</i> _{zz}
1c	91	<3	2.00 56	2.00 56	2.00 31
2c	55	3	2.00 50	2.00 44	2.00 54
3c	60	4	2.00 58	2.00 40	2.00 45
4c	66	4	2.00 58	2.00 39	2.00 43
5c	101				
4d ^a	22	0	2.00 42	2.00 42	2.00 55
5d ^a	63	0			

^a Quartet-state triradicals.

in the radicals are small as well,³ admixture as a result of off-diagonal hyperfine terms is insignificant. Thus, there is virtually no coupling between the electron and nuclear spins in the $M_S = 0$ state, and the ν_p line width does not contain contributions stemming from electron-nuclear interactions. Electron spin lattice relaxation which can be responsible for nonsecular (T_1) contributions (i.e., lifetime broadening) to the ENDOR line width is obviously slow enough ($T_{1e} \gg 2 \times 10^{-5}$ s) in the rigid matrix to not mask this drastic line-narrowing effect.

By selectively pumping the ESR transitions $\Delta M_S = \pm 1$ in the rigid matrix, the nuclear spin polarization in the $M_S = 0$ state is greatly enhanced in comparison with pure NMR in a diamagnetic state ($S = 0$). This is demonstrated by the fact that the ^{13}C signal at the free ^{13}C frequency ($\nu_C \approx 3.5$ MHz) could be detected easily even in natural abundance. The ^{13}C ENDOR line was found to be shifted to higher frequencies by about 20 kHz, obviously caused by second-order hyperfine interactions of the contributing ^{13}C nuclei in different molecular positions. This assumption could be established by a recent ENDOR study on ^{13}C -labeled Yang's biradical (central carbon).⁴ The experimentally obtained significant frequency shift of about +110 kHz was shown to be in good agreement with the calculated second-order hyperfine shift $\Delta\nu = (a^2/2\nu_e)S(S+1)$ for a triplet system ($S = 1$) in the $M_S = 0$ state.

As pointed out before, the ν_p signal line width does not depend on the position in the ESR spectrum that is pumped by the microwave field. However, the signal amplitude is found to vary strongly as the magnetic field is moved through the ESR spectrum. To investigate this behavior in more detail the ENDOR-induced ESR spectra⁵ of the biradicals in frozen solution were recorded.

Rigid-Matrix ENDOR-Induced ESR Measurements. ENDOR-induced ESR spectra are obtained by setting the radio frequency on a suitable NMR transition (in this case the ν_p peak) and recording the variations in the amplitude of the ENDOR signal as the field is swept through the entire ESR spectrum. In recording the spectra, the radio-frequency source (HP 8660 B frequency synthesizer) was programmed to hold ν_p on resonance. No Zeeman modulation is applied in the recording of ENDOR, TRIPLE, and ENDOR-induced ESR spectra so that the latter appear as undifferentiated absorption lines.

Figure 2 shows the ENDOR-induced ESR spectrum of Yang's biradical **1c** in toluene at 140 K. For comparison, the figure includes also the first-derivative ESR spectrum and the integrated ESR spectrum. The peak in the center of the ESR spectrum is due to the presence of monoradicals. These do not contribute to the ν_p signal so that the ENDOR-induced ESR spectrum does not show the center peak. A similar ENDOR-induced ESR spectrum also shown in Figure 2 is obtained using the (natural-abundance) ^{13}C ENDOR signal. This spectrum is due to molecules which incorporate at least one ^{13}C nucleus. The poor signal-to-noise ratio prevents a careful comparison of the two ENDOR-induced ESR spectra.

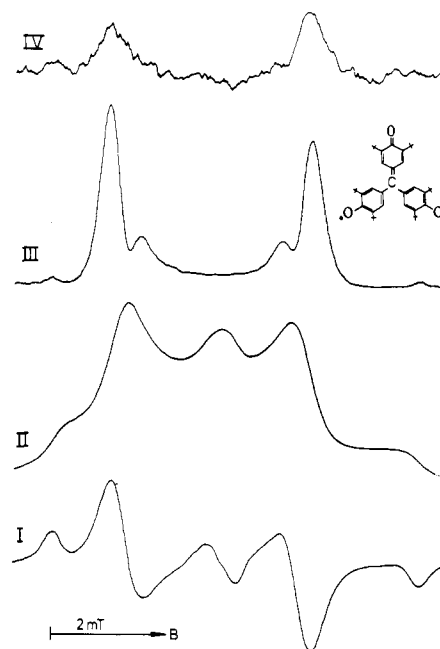


Figure 2. Rigid-matrix ESR and ENDOR-induced ESR spectra of Yang's biradical **1c** in toluene at 140 K: I, first-derivative ESR spectrum; II, integrated ESR spectrum; III, ENDOR-induced ESR spectrum, NMR field set on free proton frequency; IV, ENDOR-induced ESR spectrum, NMR field set on free carbon-13 frequency.

A remarkable feature of the ENDOR-induced ESR spectrum is that it is dominated by contributions of three distinct molecular orientations. As is well-known, the ENDOR signal strength does not depend merely on the number of molecules on resonance at a given field but is also affected strongly by relaxation effects.¹⁴ The effectiveness of a relaxation process can be a sensitive function of radical orientation so that there is no a priori reason that there should be a close resemblance between ENDOR-induced ESR and integrated ESR spectra. One must conclude that a strongly orientation-dependent relaxation process operates in biradical **1c** which gives rise to the single-crystal-type spectrum.

The ENDOR-induced ESR spectra of the biradicals **2c** and **3c**, reproduced in Figure 3, show the same features. The ENDOR-induced ESR spectrum of the biradical **5c** also given in Figure 3, on the other hand, has a line shape which is similar to the ESR line shape of randomly oriented biradicals, and the same is true for Yang's biradical **1c** in frozen paraffin oil (170 K).

The positions of the three pairs of peaks in the ENDOR-induced ESR spectra of **2c** and **3c** suggest strongly that the three distinct molecular orientations making the major contributions to the signals correspond to orientations where the external field **B** is directed along one of the three principal axes of the zfs tensor. The separation between the outer pairs of peaks corresponds to the value of $2D$ derived from matrix ESR spectra, whereas the E values obtained from the ENDOR-induced ESR peak positions are only slightly larger than those given by computer simulations of the ESR spectra. For instance, for **3c**, computer simulations give $E = 4$ MHz whereas the value derived from ENDOR-induced ESR is 5.6 MHz.

Accepting the suggestion that the single-crystal-type ENDOR-induced ESR spectra show a strong ENDOR effect for those orientations where **B** is parallel to one of the zfs tensor axes, the experimental data lead to the conclusion that the trigonal symmetry of Yang's biradical must be perturbed slightly so that $E \neq 0$. A careful computer analysis of the ESR line shape confirms this conclusion. ESR spectrum simulations give $D = 91$ MHz and $0 < E < 3$ MHz, while ENDOR-in-

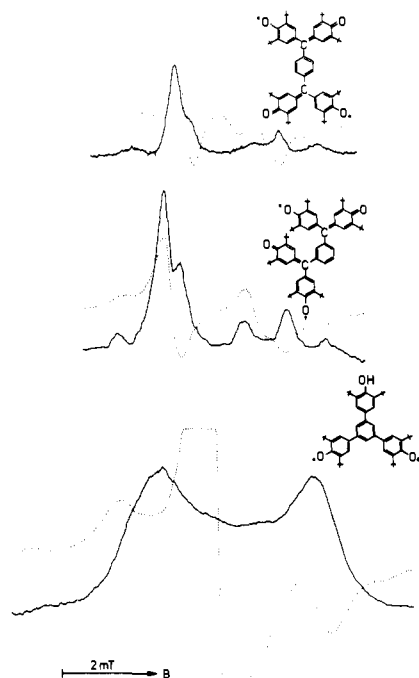


Figure 3. Rigid-matrix ESR (dotted lines) and ENDOR-induced ESR (solid lines) spectra of biradicals **2c** (top), **3c** (center), and **5c** (bottom) in toluene at 140 K.

duced ESR peak positions give $D = 91$ MHz and $E = 5$ MHz. A recently published analysis of the matrix ESR spectrum of **1c** in toluene at 77 K also concludes that the trigonal symmetry in the biradical is perturbed, with E being about 6 MHz.^{2c} Consequently, the three aryl rings must be inequivalent in rigid media, probably due to different twist angles. However, threefold symmetry appears to be retained in solution, because all six ring protons show the same hyperfine couplings within ESR and ENDOR line widths.

The close correspondence between the peak positions in the ENDOR-induced ESR spectra of the biradicals **1c**, **2c**, and **3c** and the resonance fields for molecules with a principal axis of the zfs tensor along **B** naturally leads to the conclusion that the strong anisotropy in the ENDOR effect must stem from relaxation induced by the electron-electron dipolar term. Although a detailed quantitative analysis of the phenomenon is lacking at this time, one can easily show that modulation of the zfs may be the source of the observed anisotropy.

The magnitude of the ENDOR effect depends strongly on the degree of saturation of an ESR transition¹⁷ and therefore on the electron spin relaxation time T_1 . In the biradicals considered here, it is appropriate to describe the spin system in terms of the eigenfunctions ($M_S = 1, 0, -1$) of the Zeeman interaction, since the dipolar interaction is only a small perturbation. For an arbitrary orientation of a biradical in a magnetic field, the zfs will give rise to off-diagonal elements between the 1 and 0 and the 0 and -1 (as well as the 1 and -1) spin states.¹³ Intramolecular motion, such as changes in the twist angles of the phenyl rings, will give rise to modulation of these off-diagonal terms. These fluctuations can therefore generate efficient $\Delta M_S = \pm 1$ relaxation. For the three orientations where one of the principal axes of the zfs tensor is parallel to the field, it turns out that the $M_S = 0$ state is an eigenstate of the zfs.¹³ Hence, for those three orientations zfs modulation does not give rise to $\Delta M_S = \pm 1$ relaxation. On the basis of these qualitative arguments, one can conclude that the zfs modulation indeed can induce a strongly orientation dependent T_1 process and that such a process may lead to an enhanced ENDOR effect for the three canonical orientations. Prior to recording the spectra, the microwave power, generally,

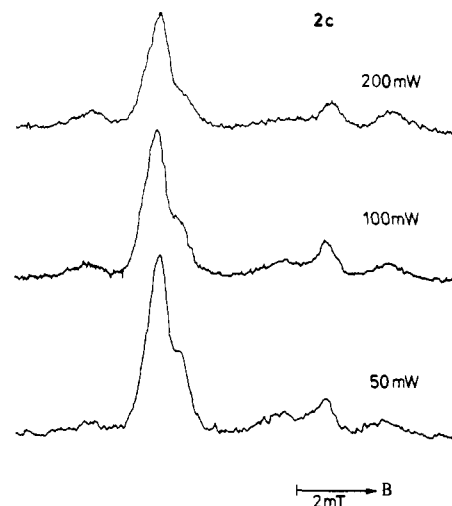


Figure 4. Rigid-matrix ENDOR-induced ESR spectra of biradical **2c** at three different microwave power levels (50, 100, 200 mW) in toluene at 140 K.

was adjusted to give an optimum ENDOR response with the field set on one of the center biradical peaks of the ESR spectrum. According to the interpretation presented above, the power setting is probably insufficient to obtain the best ENDOR response for most other orientations (T_1 is too short to give adequate saturation). The interpretation suggests, however, that as the pumping power is increased further, the relative magnitudes of the ENDOR effect for different molecular orientations will show significant changes. While the saturation behavior remains to be explored in more detail, preliminary measurements indeed confirm that the line shape of the ENDOR-induced ESR spectrum is a function of microwave power. This is illustrated in Figure 4 which shows the ENDOR-induced ESR spectrum of **2c** at three different microwave power settings.

One may expect that the molecular motion, giving rise to the anisotropy in the relaxation process, will be frozen out as the temperature is reduced. Unfortunately, toluene cannot be cooled much below 140 K without crystallization of the solvent-solute system, which invariably leads to a loss of the characteristic biradical ESR line shape. Experimental constraints prevented the cooling of MTHF below 120 K, a temperature at which the ENDOR-induced ESR spectra still exhibit single-crystal features. In paraffin oil at 170 K, however, the electron-electron dipolar relaxation process in **1c** indeed appears to be frozen out.

It should be pointed out that Davis and co-workers¹⁸ have observed powder deuterium magnetic resonance (²H NMR) spectra that exhibit a line shape that is very similar to that of the ENDOR-induced ESR spectrum of Yang's biradical **1c**. The normal axial ²H NMR powder line shape is identical with the axial biradical ESR line shape since the quadrupole and zfs Hamiltonians have the same form.¹⁹ In view of this, it is clear that modulation of the quadrupole coupling constant also can give rise to an orientation-dependent T_1 process. Since the ²H NMR powder spectra were recorded using spin echo techniques, the powder line shape could reflect such T_1 variations.

To conclude the discussion of the ENDOR experiments on triplet spin systems, it has to be pointed out that the rigid-matrix ENDOR spectrum should exhibit the free nucleus line and in addition another line placed at $\nu_N + a^T$ or at $\nu_N - a^T$ (for one kind of equivalent nuclei). The position of this second line should depend on the magnetic field setting (low-field or high-field xy or z ESR component)—which permits a selective pumping of the $|-1, M_I\rangle \leftrightarrow |0, M_I\rangle$ or $|0, M_I\rangle \leftrightarrow |1, M_I\rangle$ ESR

transition—and on the relative signs of the zfs parameter D and the respective hyperfine coupling constant. Preliminary measurements indicate that in biradical **2c** D and a^T (of the galvinoxyl meta protons) have opposite signs. Since the sign of galvinoxyl meta proton couplings is known to be positive (vide infra), the D parameter can be concluded to be negative. This is exactly what one expects for symmetry reasons. So far, however, signal-to-noise problems have prevented a systematic study of matrix ENDOR lines other than the ν_p peak. Since this method of relative sign determination has been more successful in the field of the quartet-state ENDOR experiments, it will be discussed in more detail in the triradical section.

Triradicals (Quartet-State Molecules). Fluid-Solution ENDOR Measurements. ENDOR spectra were obtained of the triradicals generated by oxidation of **4a** and **5a**. The ENDOR spectra of the mono and triradical of **4a** in fluid solution are reproduced in Figure 5. The monoradical (**4b**) spectrum gives the following hyperfine couplings: *tert*-butyl protons, 0.14 MHz; central-ring protons, 0.47 MHz; galvinoxyl ring protons average splitting, 3.74 MHz (hindered rotation induces a slight inequivalence which results in a splitting into four lines). The ENDOR spectrum of triradical **4d** exhibits three pairs of lines with splittings of 0.53, 1.24, and 3.76 MHz, with an additional line at the free proton frequency.

The triradical spectrum **4d** can be analyzed as follows: First it is noted that each unpaired electron now is delocalized over three galvinoxyl substituents ($|J| \gg |a|$), rather than confined to one as in the monoradical. The hyperfine coupling of the galvinoxyl protons therefore is expected to be about one-third of the coupling found in the monoradical, whereas the couplings of the central-ring protons should remain fairly constant. Furthermore, in a triradical each set of equivalent protons will give rise to *two pairs* of ENDOR lines due to NMR transitions within the $M_S = \pm 3/2$ and $\pm 1/2$ electron spin manifolds. With an isotropic quartet hyperfine coupling constant of a^Q these ENDOR lines can be found at $|\nu_p \pm 3/2 a^Q|$ ($M_S = \pm 3/2$ lines) and $|\nu_p \pm 1/2 a^Q|$ ($M_S = \pm 1/2$ lines). The outer pair of lines with a splitting of 3.76 MHz must therefore be assigned to the $M_S = \pm 3/2$ lines and the pair with a splitting of 1.24 MHz to the $M_S = \pm 1/2$ lines of the galvinoxyl protons. The inner pair of peaks must be assigned to the central-ring protons ($M_S = \pm 1/2$). The $M_S = \pm 3/2$ lines (expected splitting 1.59 MHz) do not show up. Finally, the “ ν_p ” peak is due to the *tert*-butyl protons which theoretically should give two pairs of lines with splittings of about 0.14 and 0.05 MHz; these splittings are not resolved (a genuine ν_p transition does not exist in a quartet spin system).

From a comparison of the hyperfine couplings of the doublet radical **4b** with those of Coppinger's radical and aryl-substituted galvinoxyls, it is evident that the spin-density distribution within the galvinoxyl moiety is essentially the same in all of these systems and can be interpreted by means of simple SCF-MO calculations.²⁸ On passing from the doublet to the triplet or quartet spin state (i.e., different oxidation steps **4b**, **4c**, and **4d**), the probability of finding *one* of the unpaired electrons in *one galvinoxyl moiety* is reduced to one-half or one-third, respectively. This in fact is reflected by the measured hyperfine couplings. The equivalence of all 12 galvinoxyl ring protons in **4d** proves that this triradical has threefold symmetry in solution (propeller shape). The spin-density distribution in the bridging phenyl ring of **4b** is approximately the same as that obtained for phenyl galvinoxyl (ortho/para positions).⁴ In contrast to the galvinoxyl parts of the molecule, the probability of finding an unpaired electron in the central ring remains unaltered in the doublet and the respective quartet spin states. Consequently, the experimentally found hyperfine couplings for the protons in the bridge are of the same magnitude in **4b** and **4d**.

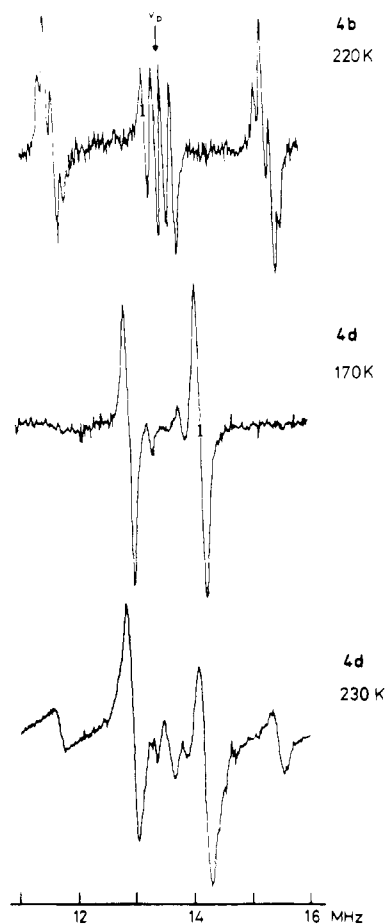


Figure 5. Fluid-solution ENDOR spectra of the first and third oxidation steps of **4a** in toluene: top; monoradical **4b**; center and bottom, triradical **4d** at 170 and 230 K, respectively (note the wings of the two spectra at about 11.5 and 15.5 MHz).

The solution ENDOR spectrum of the triradical is of considerable interest since the $M_S = \pm 3/2$ and $\pm 1/2$ ENDOR lines associated with a given set of equivalent protons exhibit quite distinct properties. As Figure 5 shows, the optimum temperature for observation of the $M_S = \pm 1/2$ lines is close to the melting point of the solvent (about 170 K in toluene). The $M_S = \pm 3/2$ lines are observed at higher temperatures (the optimum temperature in toluene is about 230 K). Moreover, much higher microwave power levels are required to optimize the $M_S = \pm 3/2$ signals than those used to observe the $M_S = \pm 1/2$ signals. Preliminary measurements have shown that a microwave power level of about 100 mW is required to saturate the $M_S = \pm 3/2$ ENDOR lines of **4d** (190 K, toluene) as compared to about 10 mW for the $M_S = \pm 1/2$ lines.

The distinct microwave power and temperature dependence can be understood by considering the effect of the electron-electron dipolar interaction. Ignoring hyperfine contributions, the energy levels in a triradical to first order are given by²⁰

$$\nu_{\pm 3/2} = \pm 3/2 \nu_e + 1/2 D(3n^2 - 1) \quad (1)$$

$$\nu_{\pm 1/2} = \pm 1/2 \nu_e - 1/2 D(3n^2 - 1) \quad (2)$$

where ν_e is the Zeeman interaction, D is the zfs constant, and n is the direction cosine of the molecular symmetry axis with respect to the field direction. These equations show that the resonance condition for two of the three allowed ESR transitions in fluid solution is affected by the anisotropy of the dipolar interaction. This modulation has the following consequences: At low temperatures the anisotropy is not completely averaged out by the Brownian motion. The resulting broadening of that

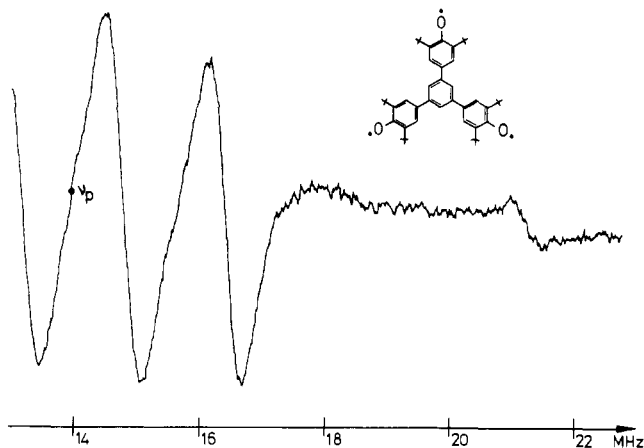


Figure 6. Part of the fluid-solution ENDOR spectrum of triradical **5d** in toluene at 190 K: Microwave power 70 mW, radio-frequency power 350 W ($B_{\text{NMR}} = 1.2$ mT in the rotating frame).

part of the ESR spectrum due to the $|^3/2\rangle \leftrightarrow |^1/2\rangle$ and $|^{-1/2}\rangle \leftrightarrow |^{-3/2}\rangle$ transitions is associated with a decrease in the $M_S = \pm 3/2$ ENDOR signal intensity. A similar broadening mechanism operates in biradicals where it is also found that the conditions for observing ENDOR improve toward higher temperatures where the zfs is increasingly averaged out.³ On the other hand, eq 1 and 2 show that the resonance field for the $|^{-1/2}\rangle \leftrightarrow |^1/2\rangle$ ESR transition is not affected by the dipolar interaction. As a consequence, the ENDOR signals detected via this ESR line can be expected to show a temperature dependence which is very similar to that of a monoradical; e.g., the maximum effect should be found close to the melting point of the solvent.^{14,17} Apart from this T_2 effect on the ENDOR signal strength, one also has to consider its dependence on the electron spin lattice relaxation time T_1 . Modulation of the dipolar interaction by the molecular tumbling gives rise to $\Delta M_S = \pm 1, \pm 2$ relaxation processes between all levels except between the $|^1/2\rangle$ and $|^{-1/2}\rangle$ spin states.²¹ This results in a distinct saturation behavior of the $|^{-3/2}\rangle \leftrightarrow |^{-1/2}\rangle$ and $|^1/2\rangle \leftrightarrow |^3/2\rangle$ ESR transitions on the one hand and the $|^{-1/2}\rangle \leftrightarrow |^1/2\rangle$ transition on the other hand. Specifically, one predicts that the latter transition will saturate at lower microwave power levels (longer T_1) than the former two transitions. As a consequence, the optimum $M_S = \pm 1/2$ ENDOR signal will be obtained at a lower microwave power level than is required for the $M_S = \pm 3/2$ ENDOR lines.

The monoradical ENDOR spectrum of **5b** shows three pairs of peaks, and the hyperfine coupling constants are given in Table II with the signs derived from TRIPLE experiments. In the six-line ESR spectrum only the average of the large splittings (~ 4.8 MHz) due to five nearly equivalent protons can be measured.^{2a} The accidental degeneracy of the hyperfine splittings of the two phenoxyl and of two of the central-ring protons is lifted in the ENDOR spectrum by using nematic phase IV liquid crystal as solvent.

As before, it may be assumed that the hyperfine couplings of the central-ring protons will remain relatively constant upon further oxidation, whereas the phenoxyl-ring proton coupling will be reduced by about a factor of 3. In the triradical ENDOR spectrum of **5d** (Figure 6) three pairs of lines show up, their assignment being given in Table II. Accidentally the $M_S = \pm 1/2$ ENDOR signals of the central-ring protons and the $M_S = \pm 3/2$ signals of the phenoxyl protons have roughly identical positions. Due to the relatively large value of the zfs parameter of 63 MHz—as compared to 22 MHz in **4d**—the outer lines can only be observed as very weak broad resonances when applying high microwave power (~ 100 mW) and when carefully optimizing the temperature at which the spectrum

Table II. Hyperfine Coupling Constants of Monoradical **5b** and Triradical **5d**^a

proton	5b <i>a</i> , MHz	5d <i>a</i> ^Q , MHz	5d resonance positions	
			$M_S = \pm 1/2$	$M_S = \pm 3/2$
<i>tert</i> -butyl	+0.17			
central-ring ortho	-4.63	-4.90	11.6, 16.4	6.8, 21.2
central-ring para	-4.92	-4.90		
phenoxyl ring	+4.63	+1.62	13.2, 14.8	11.6, 16.4

^a All hyperfine coupling constants are measured by ENDOR, accurate within ± 0.01 MHz (**5b**: MTHF, 220 K; **5d**: toluene, 190 K). Additionally, the approximate ENDOR line positions (in MHz) of **5d** are given ($\nu_p \approx 14.0$ MHz).

is recorded. In fact, these peaks would have escaped detection were it not for the fact that their position as well as the optimum conditions for their detection could be predicted beforehand.

The measured hyperfine couplings for the monoradical **5b** compare well with those of analogous phenoxyl radicals²⁹ indicating a similar spin-density distribution. It is noteworthy that the spin populations in the meta positions of the phenoxyl ring and the ortho/para positions of the central ring have nearly the same absolute value but opposite signs. The positive signs of the latter are reasonable because the central ring is attached to the para position of the phenoxyl ring. As is well-known, the spin population in the para position of the phenoxyl moiety is positive whereas it is negative in the meta positions. The different spin-density distributions found in the doublet (**5b**) and quartet (**5d**) spin states can be interpreted analogously to **4b/4d** (vide supra).

The presence of the $M_S = \pm 3/2$ lines in the ENDOR spectrum of a triradical and the ease with which these lines can be identified using their temperature and saturation behavior make the ENDOR method a suitable tool for the identification of quartet-state radicals with small D values of about 20–60 MHz. An alternative magnetic resonance method is the detection of the $\Delta M = 3$ resonance line in the matrix ESR spectrum.²² If the triradical has a small D value, the detection of the $\Delta M = 3$ line may be hard if not impossible for intensity reasons,²² whereas the ENDOR detection of the $M_S = \pm 3/2$ lines under those conditions will be a simple matter. On the other hand, if D is large the ENDOR method obviously poses serious problems and ESR detection of the $\Delta M = 3$ line may be a feasible alternative.

Although all of the experimental results can readily be explained by assuming the quartet state to be the ground state of both triradicals under investigation, it has to be pointed out that, for instance, in **4c** the doublet–quartet splitting only amounts to about 90 J/mol.⁸ Hence, the two doublet states of the triradical should be thermally populated and might therefore show up in the ENDOR spectrum. From quantum mechanical calculations it is known²³ that the degeneracy of the two doublet states is lifted by the hyperfine interaction resulting in a very complex energy level diagram. In our ENDOR experiments no resonance absorption of the triradical doublet state could be detected, since all ENDOR lines could unambiguously be assigned to the quartet-state species.

Fluid-Solution TRIPLE Measurements. The effect of the modulation of the electron–electron dipolar interaction is also observed in TRIPLE spectra of triradical **4d** in fluid solution. Figure 7 shows that the application of a strong radio-frequency field (~ 0.6 mT in the rotating frame) at one of the ENDOR line positions results in a reduction in intensity of the lines on the same side of ν_p and an increase in intensity of the three lines on the other side. The magnitude of this effect depends strongly on whether one of the $M_S = \pm 3/2$ lines or one of the $M_S = \pm 1/2$ lines is pumped. The experimental results for various possible combinations of pump and scan frequencies are collected in

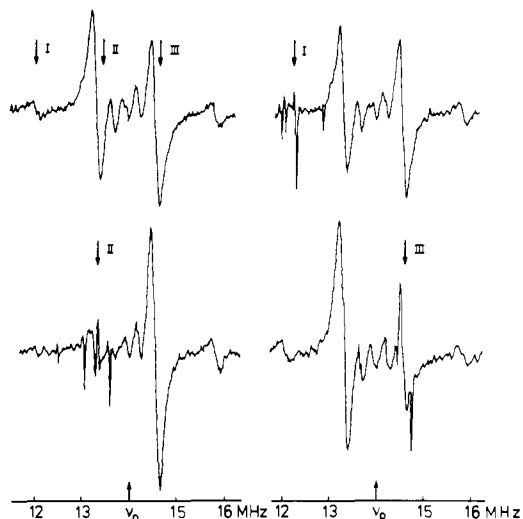


Figure 7. Fluid-solution ENDOR and TRIPLE spectra of triradical **4d** in toluene at 190 K; top left: ENDOR spectrum of **4d**. The arrows indicate the setting of the pump frequency to give the respective TRIPLE spectra I, II, and III (for more experimental details, see text).

Table III. Experimental and Theoretical (in Parentheses) ENDOR and TRIPLE Amplitudes (Relative Units) of Triradical **4d**

NMR scan freq, MHz	NMR pump off (ENDOR)	NMR pump on freq, MHz		
		12.1	13.3	14.6
12.1 $ M_S\rangle = 3/2$	0.17 (0.24)		0.08 (0.19)	0.26 (0.30)
13.3 $ M_S\rangle = 1/2$	1.0 (1.0)	0.9 (0.9)		1.5 (1.2)
14.6 $ M_S\rangle = 1/2$	1.0 (1.0)	1.1 (1.1)	1.5 (1.2)	
15.8 $ M_S\rangle = 3/2$	0.17 (0.24)	0.17 (0.24)	0.26 (0.30)	0.12 (0.19)

Table III. All of the dominant features observed in the ENDOR and TRIPLE spectra are well reproduced by a computer simulation based on a general density-matrix treatment of multiresonance effects in ESR spectra²⁴ analogous to the theory of saturation and double-resonance effects in ESR spectra developed by Freed.²⁵ Modulation of the zero-field and dipolar hyperfine splittings by the rotational Brownian motion were taken to be the only sources of relaxation. The actual input parameters were: rotational correlation time $\tau_c = 5 \times 10^{10}$ s, $\text{Tr}(A^2) = 10 \text{ MHz}^2$, $\text{Tr}(D^2) = 2/3 D^2 = 330 \text{ MHz}^2$, $a_{\text{iso}} = 1.2 \text{ MHz}$, $B_2(\text{NMR pump}) = 0.48 \text{ mT}$, $B_2(\text{NMR scan}) = 0.40 \text{ mT}$, and $B_1(\text{ESR}) = 0.0014 \text{ mT}$. The results of the simulation are also given in Table III for direct comparison with the experimental data. Clearly the theoretical results are in quite good agreement with the experimental findings.

Rigid-Matrix Measurements. The ESR spectrum of a triradical in glassy solution is characterized by a biradical-type line shape in the wings and a relatively narrow line in the center;²⁶ see Figure 8. The "biradical line shape" is due to the zfs-dependent $| -3/2 \rangle \leftrightarrow | -1/2 \rangle$ and $| 1/2 \rangle \leftrightarrow | 3/2 \rangle$ transitions. The narrow line at $g \approx 2$ stems from the $| -1/2 \rangle \leftrightarrow | 1/2 \rangle$ transition, which, as mentioned before, is not affected by the zfs. As pointed out before, the three distinct contributions to the rigid-matrix spectrum provide a unique opportunity to probe the ENDOR effect within different electron spin manifolds and for different radical orientations. Figure 8 shows the ENDOR spectra of **4d** for the magnetic field set at three different positions of the matrix spectrum. With the field set on

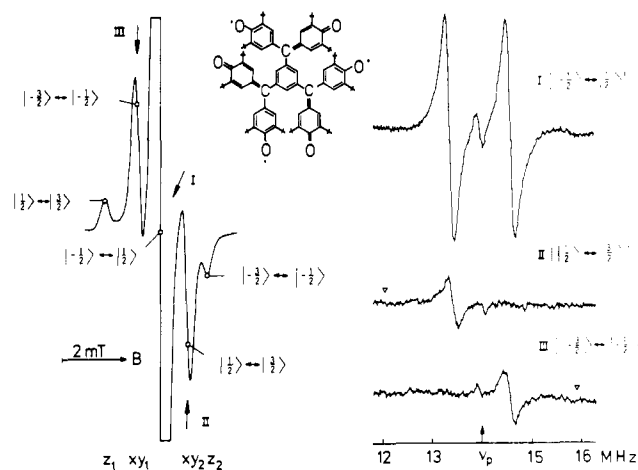


Figure 8. Experimental rigid-matrix ESR (left) and ENDOR (right) spectra of triradical **4d** in toluene; microwave power 40 mW, radio-frequency power 100 W ($B_{\text{NMR}} = 0.62 \text{ mT}$ in the rotating frame). The arrows indicate the respective ESR component pumped in the ENDOR experiment; the marks (∇) indicate the NMR frequencies where the ENDOR lines in the $M_S = \pm 3/2$ manifolds should, if at all, show up.

the center peak, the ENDOR spectrum consists of a pair of peaks with a separation of 1.23 MHz (line width 190 kHz) and a peak close to the free proton frequency which may be attributed to the *tert*-butyl protons. The positions of the dominant peaks correspond exactly to the positions of the major peaks (width 90 kHz) in the fluid solution ENDOR spectrum. In the latter spectrum the peaks were assigned to the $M_S = \pm 1/2$ NMR transitions of the galvinoxyl ring protons. In the rigid matrix, the ESR transition being pumped with the field set in the center of the spectrum is predominantly the $| -1/2 \rangle \leftrightarrow | 1/2 \rangle$ transition. Hence, the $M_S = \pm 1/2$ lines are expected to dominate the ENDOR spectrum, as is indeed found experimentally. The increased line width may account for the failure to observe the $M_S = \pm 1/2$ lines of the central-ring protons.

The $| -3/2 \rangle \leftrightarrow | -1/2 \rangle$ or $| 1/2 \rangle \leftrightarrow | 3/2 \rangle$ resonance can be pumped selectively by setting the magnetic field on the high-field or low-field part of the "biradical-type" spectrum. Figure 8 also illustrates the ENDOR spectra that are obtained with the field adjusted so that the microwave field primarily saturates the $| -3/2 \rangle \leftrightarrow | -1/2 \rangle$ transition or the $| 1/2 \rangle \leftrightarrow | 3/2 \rangle$ transition of those molecules which are oriented so that the molecular plane is approximately parallel to the field direction (xy orientation). It is noted that under those conditions we observe only the low-frequency peak (field set on the high-field xy component of the ESR spectrum) or the high-frequency peak of the pair observed before. This is, of course, the expected behavior. For an off-center setting of the field, one preferentially saturates a particular ESR transition depending on the fine-structure component selected and the sign of the zfs parameter D . If this is the $| -3/2 \rangle \leftrightarrow | -1/2 \rangle$ transition, one can observe only the $M_S = -3/2$ and $-1/2$ ENDOR lines which, depending on the sign of the hyperfine coupling, will be found either below ν_p ($a < 0$) or above ν_p ($a > 0$) (vide infra). Under the present conditions the $M_S = \pm 3/2$ lines are apparently too broad and weak to be observable.

The ENDOR line width in the three spectra is constant and only about twice the fluid-solution line width. With the chosen center and off-center field settings a range of radical orientations is expected to contribute to the ENDOR signals and it is clear that anisotropy in the hyperfine splitting of the galvinoxyl protons would give rise to a significant broadening of the resonance lines if the molecular motion is truly frozen out under the experimental conditions ($\sim 140 \text{ K}$, toluene). The experimental results inevitably lead to the conclusion that

whereas molecular motion is sufficiently slow to give a rigid-matrix triradical spectrum (rotational correlation time long compared to the inverse of the zfs), it is fast enough to practically average out the anisotropic part of the hyperfine interaction. With a zfs of about 20 MHz and with the assumption of anisotropic contributions of the same order as the isotropic hyperfine coupling, the results indicate that the rotational correlation time must be somewhere between 10^{-6} and 10^{-8} s.

From eq 1 and 2 for the four electron spin energy levels in a triradical, one can deduce that, with the symmetry axis perpendicular to the field direction (*xy* orientation), the $|1/2\rangle \leftrightarrow |3/2\rangle$ resonance will give rise to a strong peak on the high-field side of the center of the spectrum if $D > 0$. The $|-3/2\rangle \leftrightarrow |-1/2\rangle$ resonance is found as a strong peak on the low-field side under those conditions. The situation is reversed if $D < 0$. The zfs parameter D is given by²⁶

$$D = \frac{3}{4}(g^2\beta^2/h)\langle(1/r_{12}^3) - (3z_{12}^2/r_{12}^5)\rangle \quad (3)$$

where r_{12} is the distance vector between any two unpaired electrons and z_{12} is the component of this vector along the symmetry axis in **4d**. The formula shows that in biradicals and triradicals with axial symmetry $D > 0$ because the symmetry axis lies perpendicular to r_{ij} , i.e., $z_{ij} = 0$ (or at least to the extent that $3\langle z_{ij}^2/r_{ij}^5 \rangle \ll \langle 1/r_{ij}^3 \rangle$).

Pumping of the $|1/2\rangle \leftrightarrow |3/2\rangle$ transition yields the low-frequency ENDOR signal while pumping of the $|-3/2\rangle \leftrightarrow |-1/2\rangle$ transition yields the high-frequency ENDOR line; see Figure 8. In the former case, a set of equivalent protons will give an ENDOR response by pumping the NMR transition in the $M_S = 1/2$ state at the frequency $\nu = \nu_p - 1/2a^Q$, where a^Q in our case is the isotropic hyperfine coupling constant of the galvinoxyl meta protons. For $a^Q > 0$ this ENDOR signal will be found at the low-frequency side of ν_p , whereas it will be on the high-frequency side for $a^Q < 0$. The spectra shown in Figure 8 establish that D and a^Q have the same sign so that a^Q must be positive. This conclusion that $a^Q > 0$ is confirmed by our TRIPLE resonance measurements. Moreover, this is consistent with NMR studies on Coppinger's radical ("galvinoxyl") and Yang's biradical (**1c**) clearly indicating a positive sign of the meta proton coupling constant in these doublet and triplet spin systems, respectively.²⁷

Whereas D is expected to be positive in the axially symmetric triradicals **4d** and **5d**, D is expected to be negative in the biradicals **4c** and **5c** because the unpaired electrons can be viewed to be localized on roughly opposite sides of the molecule and the maximum dipolar interaction will now be found if the vector connecting the centers of gravity of the two electron charge distributions (z_{12} in eq 3) is aligned along the field. It is of interest that the change in sign of D going from biradicals **c** to the triradicals **d** is reflected in the matrix ESR spectra of these species.

The matrix ESR spectra of the biradical **5c** and the triradical **5d** exhibit an asymmetry that is introduced by the anisotropy of the g tensor. For the biradical the analysis gives $g_{zz} > g_{xx}, g_{yy}$, whereas for the triradical $g_{zz} < g_{xx} = g_{yy}$.^{2a} This reversal of the g -value-induced asymmetry is a strong indication that the z axis is turned out of the molecular plane upon going from the biradical to the triradical oxidation stage. An analogous effect is found in the matrix spectra of the second (**4c**) and third (**4d**) oxidation steps of **4a**. In that case, however, $g_{zz} \approx g_{yy} < g_{xx}$ for the biradical and $g_{zz} > g_{xx} = g_{yy}$ for the triradical (see Table I). The difference between the g factors of the two compounds probably can be attributed to a difference in the degree of planarity of the molecules.

Conclusions

In conclusion we want to state that ENDOR in liquid solution as well as in rigid media can be extended to triplet and

quartet spin systems. Besides the well-known resolution enhancement obtained on passing from ESR to ENDOR, the ENDOR technique yields the following additional advantages when applied to the field of organic multispin systems:

(i) **Biradicals.** The rigid-matrix ENDOR spectroscopy of biradicals provides the opportunity of studying a paramagnetic species in the "diamagnetic" $M_S = 0$ spin state resulting in an ENDOR line at the free nuclear frequency with an unusually small line width of ~ 20 kHz. The sensitivity gain in comparison to NMR—obtained by "quantum transformation"—is clearly demonstrated by the fact that the free carbon-13 frequency line could readily be detected even in natural abundance.

(ii) **Triradicals.** In the liquid-solution measurements of triradicals ENDOR offers the unique possibility of selecting either the ESR transitions $|-1/2\rangle \leftrightarrow |1/2\rangle$ or $|-3/2\rangle \leftrightarrow |-1/2\rangle$ and $|1/2\rangle \leftrightarrow |3/2\rangle$ in one species for studying hyperfine interactions or relaxation processes. The former transition which is independent of the electron-electron dipolar interaction exhibits typical "monoradical" behavior, while the latter, which are affected by this interaction, could be shown to behave like a biradical.

(iii) **Bi- and Triradicals.** Rigid-matrix ENDOR has proved to be of particular value in the determination of the relative signs of the zero-field splitting and the hyperfine splitting parameters of multispin states.

Acknowledgments. The authors thank Dr. J. Reusch for supplying the galvinoxyl samples. This work was supported by the Deutsche Forschungsgemeinschaft (Grants SFB 161 and DFG Normalverfahren). H.K. is grateful to the Fonds der Chemischen Industrie for financial support. H.v.W. thanks the Freie Universität Berlin for a 2-month fellowship and gratefully acknowledges the friendship and hospitality extended by staff and students of the Institut für Molekülphysik and the Institut für Organische Chemie.

References and Notes

- (1) (a) Institut für Organische Chemie. (b) Institut für Molekülphysik.
- (2) (a) C. Nowak, G. Kothe, and H. Zimmermann, *Ber. Bunsenges. Phys. Chem.*, **78**, 265 (1974); (b) W. Broser, B. Kirste, H. Kurreck, J. Reusch, and M. Plato, *Z. Naturforsch., B*, **31**, 974 (1976); (c) K. Mukai, T. Mishina, and K. Ishizu, *J. Chem. Phys.*, **66**, 1680 (1977); (d) G. Kothe, A. Naujok, and E. Ohmes, *Mol. Phys.*, **32**, 1215 (1976); G. Kothe, *ibid.*, **33**, 147 (1977).
- (3) H. van Willigen, M. Plato, K. Möbius, K. P. Dinse, H. Kurreck, and J. Reusch, *Mol. Phys.*, **30**, 1359 (1975).
- (4) B. Kirste, H. Kurreck, W. Lubitz, and K. Schubert, *J. Am. Chem. Soc.*, **100**, 2292 (1978).
- (5) B. H. Robinson, L. A. Dalton, A. H. Beth, and L. R. Dalton, *Chem. Phys.*, **18**, 321 (1976).
- (6) K. P. Dinse, R. Biehl, and K. Möbius, *J. Chem. Phys.*, **61**, 4335 (1974); R. Biehl, M. Plato, and K. Möbius, *J. Chem. Phys.*, **63**, 3515 (1975).
- (7) W. Harrer, H. Kurreck, J. Reusch, and W. Gierke, *Tetrahedron*, **31**, 625 (1975).
- (8) W. Gierke, W. Harrer, B. Kirste, H. Kurreck, and J. Reusch, *Z. Naturforsch., B*, **31**, 965 (1976).
- (9) The tris(phenol) **5a** was a gift from Dr. G. Kothe, Universität Freiburg, Freiburg, West Germany, which is gratefully acknowledged.
- (10) R. Biehl, W. Lubitz, K. Möbius, and M. Plato, *J. Chem. Phys.*, **66**, 2074 (1977).
- (11) H. D. Brauer, H. Stieger, J. S. Hyde, L. D. Kispert, and G. R. Luckhurst, *Mol. Phys.*, **17**, 457 (1969).
- (12) W. Vollmann, *Mol. Phys.*, **32**, 395 (1976); Thesis, FU Berlin, 1977.
- (13) E. Wasserman, L. C. Snyder, and W. A. Yager, *J. Chem. Phys.*, **41**, 1763 (1964).
- (14) M. Plato, R. Biehl, K. Möbius, and K. P. Dinse, *Z. Naturforsch., A*, **31**, 169 (1976).
- (15) J. S. Hyde, G. H. Rist, and L. E. Göran Eriksson, *J. Phys. Chem.*, **72**, 4269 (1968).
- (16) G. H. Rist and J. S. Hyde, *J. Chem. Phys.*, **52**, 4633 (1970).
- (17) R. D. Allendoerfer and A. H. Makl, *J. Magn. Reson.*, **3**, 396 (1970).
- (18) J. H. Davis, K. R. Jeffrey, M. Bloom, and M. J. Valic, Proceedings of the 172nd American Chemical Society Meeting, San Francisco, Calif., 1976.
- (19) A. Abragam, "The Principles of Nuclear Magnetism", Clarendon Press, Oxford, 1961; K. Abdollah, E. E. Burnell, and M. I. Valic, *Chem. Phys. Lipids*, **20**, 115 (1977).
- (20) K. Reibisch, G. Kothe, and J. Brickmann, *Chem. Phys. Lett.*, **17**, 86 (1972).
- (21) A. Carrington and G. R. Luckhurst, *Mol. Phys.*, **8**, 125 (1964).
- (22) S. I. Weissman and G. Kothe, *J. Am. Chem. Soc.*, **97**, 2537 (1975).

- (23) A. Hudson and G. R. Luckhurst, *Mol. Phys.*, **13**, 409 (1967).
 (24) M. Plato, to be submitted for publication.
 (25) J. H. Freed, *J. Chem. Phys.*, **43**, 2312 (1965).
 (26) J. Brickmann and G. Kothe, *J. Chem. Phys.*, **59**, 2807 (1973).
 (27) R. W. Kreilick, *Mol. Phys.*, **14**, 495 (1968); P. W. Kopf and R. W. Kreilick,

- J. Am. Chem. Soc.*, **91**, 6569 (1969).
 (28) G. R. Luckhurst, *Mol. Phys.*, **11**, 205 (1966); K. Mukai, T. Kamata, T. Tamaki, and K. Ishizu, *Bull. Chem. Soc. Jpn.*, **49**, 3376 (1976).
 (29) K. Scheffler and H. B. Stegmann, "Elektronenspinresonanz", Springer-Verlag, Berlin, 1970, p 339 ff, and references cited therein.

Perturbation Theory, 3-Orbital-4-Electron and 4-Orbital-4-Electron Bonding, and the Inductive Effect in Tetrahedral Compounds

Evgeny Shustorovich¹

Contribution from the Department of Chemistry, Cornell University, Ithaca, New York 14853. Received March 2, 1978

Abstract: The 3-center-3-orbital-4-electron (3c-3o-4e) and 3-center-4-orbital-4-electron (3c-4o-4e) bonding in the linear molecules (fragments) $L'-E-L$ have been considered by first-order perturbation theory (E is a transition metal M or main group element A atom). The difference in ligand orbital energies $\delta\alpha' = \alpha(L') - \alpha(L)$ was taken as a perturbation when in the initial symmetric $L-E-L$ molecule a ligand L was substituted by a ligand L' . It was shown that in the 4o-4e case the s (or sd_σ) and p contribution to changes in the E-L bond overlap population, $\delta N(E-L)/\delta\alpha'$, are always of the opposite signs, the s (or sd_σ) one negative and the p one positive. As the former contribution is usually larger in absolute value than the latter one, for $\delta\alpha' > 0$ (L' is a better donor than L) the E-L bond will be weakened as compared with that in the initial symmetric $L-E-L$ species. This result was generalized for 4o-4e bonding embracing any number of centers (ligands) which makes it applicable to many complexes, and in particular to tetrahedral $AL_{4-k}L'_k$ and planar trigonal $AL_{3-k}L'_k$. It was proved that the first-order effects in $AL_{m-k}L'_k$ are additive, which explains the nature and main regularities of the inductive effect and the mutual influence of ligands (MIL) in compounds in question. In particular, the dependence of the A-L bond strength on the number and the electronegativity of L' as well as Bent's rules concerning the central atom rehybridization has been represented in explicit form. It was shown that in the orbitally deficient 3o-4e case there is only a negative contribution to the E-L bond overlap population, so that for a better donor L' the E-L bond will always be weakened and much more than in the 4o-4e case. This weakening must take place regardless of the nature of the central atom orbital (s, p, or d) or the type of bonding (σ or π). This result was also generalized for many-center cases, which is especially important for some hypervalent complexes of the AL_m type ($m = 5-7$). The nodal structures of the canonical MOs for all these cases were obtained permitting a visual explanation of the MIL and, in particular, the trans influence. The results obtained agree with the experimental and computational data and permit a number of predictions to be made.

Introduction

One of the most important questions in which a chemist is interested is how the E-L bonds are changed in substituted derivatives $EL_{m-k}L'_k$ as compared with the initial compound EL_m . From this point of view it is useful to divide all the polyhedra EL_m into two groups depending on whether or not all the ligands L are geometrically equivalent with respect to the substituent L' . The first group includes, for instance, the linear $L'-E-L$, planar trigonal EL_2L' , and tetrahedral EL_3L' molecules; the second includes, for instance, square EL_3L' , trigonal bipyramidal EL_4L' , octahedral EL_5L' , and pentagonal bipyramidal EL_6L' compounds. In the course of our work to develop the perturbation MIL theory for all types of polyhedra^{2,3} we found that the first group is not only simpler to consider but can be combined on the basis of 4o-4e bonding. On the other hand, we found that the orbitally deficient 3o-4e bonding represents the universal basis for a great variety of hypervalent molecules, from XeF_2 to IF_7 .

It should be added that the linear molecules $L'-E-L$ have been theoretically studied mainly for the symmetric case $L' = L^4$ but until now there has been no analytical consideration of the unsymmetrical case $L' \neq L$ (see the last section of this work). Besides the linear case, it is even more interesting to consider general properties of the 4o-4e and 3o-4e bonding to establish those which do not depend on the number of centers (ligands). This can shed light on the nature of the trans influence in coordination compounds $EL_{m-1}L'$ where the largest changes (as compared with EL_m) take place within the linear

fragment $L'-E-L$.⁵ Finally, as the effects of substitution in polyhedra of the first group (due to their isotropy) can be reduced to manifestations of the inductive effect, especially well studied for tetrahedral molecules $AL_{4-k}L'_k$, we can understand its nature along the same lines.

Formulation of the Objective

The purpose of the present work is to develop the first-order perturbation theory of the 4o-4e and 3o-4e bonding for any number of centers and on this basis to consider the effects of substitution (the inductive effect) in linear, planar trigonal, and tetrahedral molecules, as well as possible applications of this theory to some polyhedra of the second group (the comprehensive perturbation MIL theory of these polyhedra will be given in the subsequent paper³).

As a perturbation we shall use the difference in ligand orbital energies, i.e., diagonal matrix elements (Coulomb integrals).

$$\langle \chi_{L'} | H | \chi_{L'} \rangle - \langle \chi_L | H | \chi_L \rangle = \delta\alpha' \quad (1)$$

Our criterion for the E-L bond strength is the overlap population $N(E-L)$ in the form

$$N(E-L) = \sum_i^{\text{occ}} \sum_m c_{im} c_{iL} S_{mL} \quad (2)$$

Here c_{im} and c_{iL} stand for the coefficients in the canonical MOs, ψ_i ,